Math. Model. Nat. Phenom. 20 (2025) 16
https://doi.org/10.1051/mmnp/2025014

Mathematical Modelling of Natural Phenomena
www.mmnp-journal.org

PREDATOR FUNCTIONAL RESPONSE IN MATHEMATICAL MODELS COMPARED TO THE ZOOPLANKTON FUNCTIONAL RESPONSE IN A LAKE ECOSYSTEM

Nailya I. Nurieva[1], Yuri V. Tyutyunov[2], Nikolay S. Minayev[1],
Dmitry A. Tikhonov[1,3], Ignat S. Minayev[1],
Nataly P. Radchikova[1,4], Alexey V. Rusakov[1],
Boris V. Adamovich[1,5] and Alexander B. Medvinsky[1,*]

Abstract. The problem of predator interference and the associated choice between two types of functions describing the functional response in mathematical modeling of population dynamics are widely discussed. It is the choice between predator-dependent and prey-dependent functions. Here we present the results of comparing a wide range of the functions describing the functional response, which are used in modeling trophic interactions, with the functional response that is characteristic of interactions between phytoplankton and zooplankton populations in the ecosystem of the Naroch Lakes (Belarus). We apply the knowledge-and-data-driven, or KDD, approach, which allows us to use the results of the monitoring of the Naroch Lakes ecosystem, to identify the time-dependent functional response in each of the reservoirs of this ecosystem. The KDD approach provides for direct input of monitoring data into the mathematical description of population dynamics. As a result, we show that predator-dependent functional responses best match the environmental processes in the ecosystem of the Naroch Lakes. At the same time, we have identified predator-dependent functions that meet the monitoring data even worse than prey-dependent functions.

Mathematics Subject Classification. 92D25, 92B99.

Received October 2, 2024. Accepted April 27, 2025.

Keywords and phrases: Lake ecosystem, zooplankton functional response, functional responses in mathematical models, knowledge-and-data-driven modeling.

[1] Institute of Theoretical and Experimental Biophysics, Russian Academy of Sciences, Pushchino, Serpukhov, Moscow Region, Russia.
[2] Southern Scientific Centre of the Russian Academy of Sciences, Rostov-on-Don, Russia.
[3] Institute of Mathematical Problems of Biology, Keldysh Institute of Applied Mathematics, Russian Academy of Sciences, Pushchino, Serpukhov, Moscow Region, Russia.
[4] Moscow State University of Psychology and Education, Russia.
[5] Belarusian State University, Minsk, Belarus.

[*] Corresponding author: `alexander_medvinsky@yahoo.com`

1. Introduction

One of the main problems facing ecologists is to identify the mechanisms underlying the dynamics of populations involved in trophic interactions [1–5]. The complex structure of diverse trophic webs (see [6], as an example) often prevents identification of fundamental principles that could characterize the functioning of a wide variety of population communities. This circumstance forces researchers to resort to simplifying, reducing complex natural ecological systems when modeling population dynamics in order to make the mathematical description of the ecological processes more readily understandable. Despite the fact that "the whole is something else than the sum of its parts" [3], the reductionist approach is widely used in scientific research and is sometimes even considered as the most useful way to understand the dynamics of populations [2]. In particular, this approach is often used within the framework of the knowledge-driven, or KD, paradigm, when simple mechanistic models are aimed to describe the predator-prey (consumer-resource) interactions. In the most general way, such a description can be presented in the form of the Gause–Kolmogorov model [7–9]:

$$\frac{\mathrm{d}x}{\mathrm{d}t} = G(x)x - F_1(x,y), \tag{1.1}$$

$$\frac{\mathrm{d}y}{\mathrm{d}t} = F_2(x,y). \tag{1.2}$$

In the context of predator-prey interactions, x and y can be considered as spatially averaged densities of prey and predator populations, respectively. $G(x)$ in equation (1.1) is the intrinsic prey growth rate. $F_1(x,y)$ in equation (1.1) is the function characterizing the consumption of prey by the predator per unit of time. The function $F_1(x,y)$ is usually represented as follows:

$$F_1(x,y) = \phi(x)y, \tag{1.3}$$

where $\phi(x)$ is a prey-dependent functional response, or

$$F_1(x,y) = \phi(x,y)y, \tag{1.4}$$

where $\phi(x,y)$ is a predator-dependent functional response. $F_2(x,y)$ in equation (1.2) is the function characterizing simultaneously natality and mortality of the predator.

A qualitative analysis of the solutions to equations (1.1)–(1.2) can be carried out without specifying both the functional dependencies $G(x)$, $F_1(x,y)$ and $F_2(x,y)$ and the numerical values of the parameters of these functions. The only limitation is that the functions are assumed to be continuously differentiable [8, 9]. However, when trying to link a mathematical model to a specific ecosystem, it becomes necessary to explicitly specify functions describing the growth and trophic interactions of specific populations as well as the dependences of population dynamics on environmental factors. In this case, both the number of equations and the number of model parameters can increase significantly. This situation is aggravated by the fact that in real ecosystems, unlike their representation in the form of mathematical models (see, for example, [10, 11], it is usually not possible to separate the deterministic component of population dynamics from the influence of stochastic factors. In addition, changes in the numerical values of the parameters of mathematical models can cause transformations of the basins of attraction that determine the nature of the dynamics of the system under study [12]. Unfortunately, such transformations may not always be related to the results of field measurements of the characteristics of real ecosystems. As a result, the researcher is faced with the problem of the adequacy of the model under study, or, in other words, with the problem of linking this model to reality. This problem is caused by the fact that the solutions of ecological models depend, firstly, on the choice of variables describing the state of the system (state variables), secondly, on the choice of functions describing the dynamics of these variables, and, thirdly, on the choice of numerical values of the model parameters [2].

Now, however, there is an opportunity to look at this problem from a different angle. This opportunity has been implemented by direct input of the data obtained during ecosystem monitoring into a mathematical model. This approach was designated as knowledge-and-data-driven, or KDD, modeling [13]. In this approach, the discrete time series resulting from the ecosystem monitoring are considered as solutions to the equations of population dynamics, which have the form of discrete-time equations (maps). Note that the time scale corresponding to the time step of maps usually corresponds to some characteristic time interval of the dynamics under study (see, *e.g.*, [3, 4]). However, when using the KDD approach, "reality" appears to the researcher exclusively in the form of monitoring results of the ecosystem under study (for example, in the form of time series).Therefore, the time step of the maps is completely determined by the frequency of sampling during monitoring. The KDD approach makes it possible to specify (in the form of time series) those functions on which the population dynamics depend. It is necessary therewith to take into account the structure of the equations, as well as estimates of the numerical values of the model parameters based on the results of previous observations (in our case, the number of parameters is two). An example of such a function is the time-varying growth rate of lake phytoplankton [13]. Here, we apply the KDD-approach to reveal the zooplankton functional response in the ecosystem of the Naroch Lakes (Belarus). The Naroch Lakes ecosystem includes three water bodies, Lake Batorino, Lake Myastro, and Lake Naroch, which are interconnected by channels (see Supplementary information). We show that the Bazykin–Crowley–Martin predator-dependent functional response best matches reality for the ecosystem of these lakes.

2. METHODS

2.1. The model

In this work, the KDD approach is used to identify the dynamics of the functional response of zooplankton, taking into account the discrete nature of the data obtained during monitoring of the lake ecosystem. The structure of the mathematical description of the relationship between phytoplankton and zooplankton therewith corresponds to the structure of equations (1.1)–(1.2). The corresponding discrete model has the following form:

$$\frac{\Delta P(n)}{P(n)} = G(n) - f(n)Z(n), \tag{2.1}$$

$$\frac{\Delta Z(n)}{Z(n)} = \beta f(n)P(n) - \alpha, \tag{2.2}$$

to model the dynamics of plankton in the ecosystem of the Naroch Lakes. In (2.1) and (2.2) n is the time step number, $P(n)$ and $Z(n)$ are the abundances of phytoplankton and zooplankton, respectively; $\Delta P(n) = P(n+1) - P(n)$ and $\Delta Z(n) = Z(n+1) - Z(n)$. $G(n)$ is the intrinsic phytoplankton growth rate; $f(n)$ is the trophic function that describes the intensity of zooplankton predation per unit of phytoplankton biomass; α and β are constants; α is the intensity of the decline in the zooplankton abundance unrelated to trophic interactions between zooplankton and phytoplankton, and β is the efficiency of turning the phytoplankton biomass into the zooplankton abundance. Note that although the terms 'trophic functions' and 'functional response' are usually used as synonyms, in the present work, for the sake of convenience, we define trophic function as the ratio of the functional response to the phytoplankton density. The plankton sampling and the raw data obtained from the field measurements, as well as the main characteristics of the Naroch Lakes, have been given in [13, 14]; see also Supplementary Information.

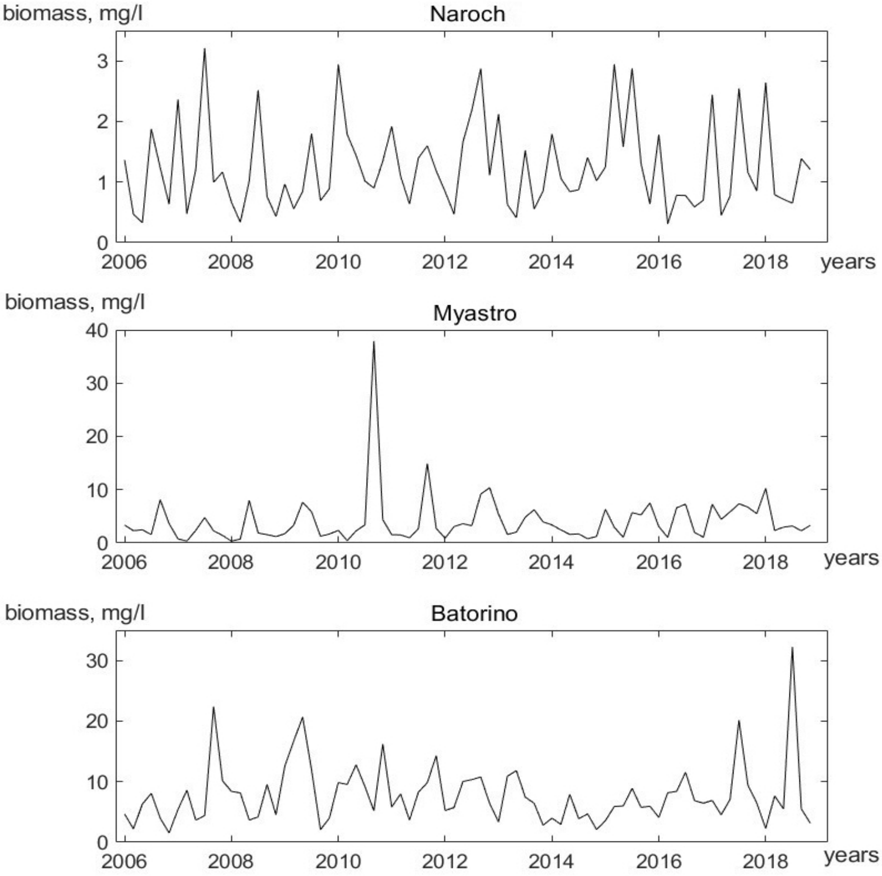

FIGURE 1. Time series plot of phytoplankton abundances in the Naroch Lakes (the time step corresponds to 1 month).

The time series (Figs. 1 and 2), which were a result of raw data processing, represent the phytoplankton oscillations $P(n)$ and the oscillations of zooplankton $Z(n)$ in each of the reservoirs of the ecosystem of the Naroch Lakes.

The irregular nature of variations in the amplitude of fluctuations in $P(n)$ in $Z(n)$ may be a manifestation of the chaotic nature characteristic of fluctuations in the abundance of lake phytoplankton [15, 16].

2.2. KDD modeling as a method for revealing the functional response

In the context of the KDD modeling, unlike the KD paradigm, it is the functions $P(n)$ and $Z(n)$ in the form of time series that are set initially [13]. Since the functions $P(n)$ and $Z(n)$ are given, it becomes possible to obtain oscillations of the trophic function $f(n)$ from (2.2) (also in the form of time series). As a next step, the dynamics of the functional response

$$\Phi(n) = f(n)P(n) \tag{2.3}$$

is compared with time series that can be obtained using formulas widely used to describe the functional response in mathematical modeling of trophic system dynamics (Tab. 1). For this comparison, we perform the following

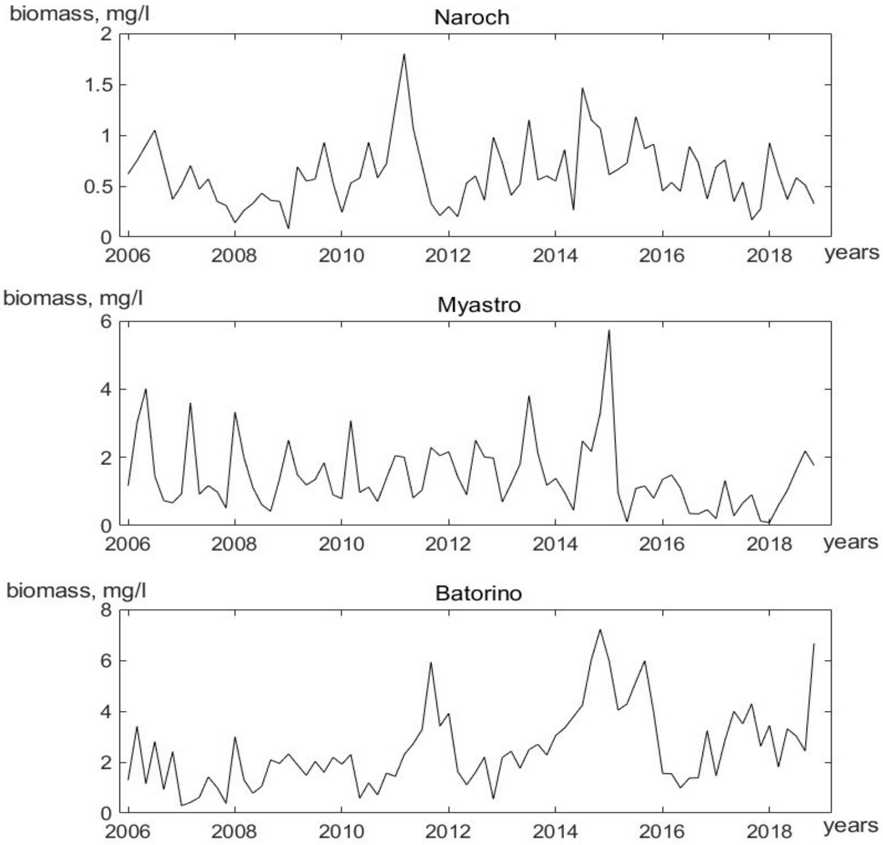

FIGURE 2. Time series plot of zooplankton abundances in the Naroch Lakes (the time step corresponds to 1 month). These time series are the result of analyzing data from monitoring of the Naroch Lakes. Samples were collected monthly at specific monitoring points at the pelagic zones of the lakes during the vegetative season (from May to October).

transformations: $x \to P(n), y \to Z(n)$ where $P(n)$ and $Z(n)$ are the phytoplankton and zooplankton time series shown in Figures 1 and 2, respectively. As a result, the functional responses $\phi(x)$ or $\phi(x, y)$ are represented as time series $\phi(n)$. The numerical values of parameters of the functions $\phi(n)$ from Table 1 are selected in such a way that the time series $\phi(n)$ correspond as well as possible to the time series $\Phi(n)$ given by equation (2.3). A method for optimizing and estimating the range of numerical values of the parameters from Table 1 is presented in subsection 2.4. Bootstrapping as a method for estimating parameter values. Now, the results of monitoring of the lake ecosystem being incorporated into $\phi(n)$ allow us to juxtapose $\phi(n)$ to $\Phi(n)$ from (2.3) in order to assess which of the functional responses, the predator-dependent or the prey-dependent, better corresponds to the plankton dynamics in the Naroch Lakes.

2.3. Correlation analysis

The Spearman correlation between variables $\phi(n)$ to $\Phi(n)$ is equal to the Pearson correlation between the rank values of these two variables:

$$\rho = \frac{cov(\phi, \Phi)}{\sigma(\phi)\sigma(\Phi)},$$

Table 1. Functional responses.

Label	Functional response $\phi(x)$ or $\phi(x,y)$	References
Linear Lotka–Volterra function	αx	Lotka, [19] Volterra, [20]
Hyperbolic function (Holling's disk equation)	$\alpha x/(1+\alpha hx)$	Holling, [21]
Exponential Ivlev function	$R(1-\mathrm{e}^{-x/a})$	Ivlev, [22]
The same, but $f(x) \to f(x/y)$ (ratio-dependent Ivlev function)	$R(1-\mathrm{e}^{-bx/y})$	Ivlev, [22]
Sigmoid function no 1	$cx^2/(d^2+x^2)$	Holling, [21]
Sigmoid function no 2	$\dfrac{cx^2}{(1+bx+chx^2)}$	Turchin, [2]
θ-Sigmoid function	$cx^\theta/(d^\theta+x^\theta)$	Holling, [21]
Mechanistic interference	$ax/(1+awy)$	Hassell, [23]
Linear interference	cx/y	Hassell & Varley, [24]
Hassell–Varley function	cx/y^m	Hassell & Varley, [24]
Hassell–Varley–Holling (HVH) function	$\dfrac{ax/y^m}{(1+awx/y^m)}$	Sutherland, [25] Arditi & Akçakaya, [26]
Beddington–DeAngelis function	$\dfrac{ax}{(1+awy+ahx)}$	Beddington, [27] DeAngelis *et al.*, [28]
Ratio-dependent Arditi–Ginzburg function	$min(ax/y, R)$	Ginzburg *et al.*, [29] Arditi *et al.*, [30]
Ratio-dependent Arditi–Ginzburg–Contois (AGC) function	$\dfrac{ax/y}{(1+ahx/y)}$	Arditi & Ginzburg, [31]
Bazykin–Crowley–Martin (BCM) function	$\dfrac{ax}{(1+ahx)} \cdot \dfrac{1}{(1+by)}$	Bazykin *et al.*, [32] Crowley & Martin, [33]
Trân function	$\frac{x}{y}(1-\mathrm{e}^{-\epsilon y})$	Trân, [34]
Tyutyunov function no 1	$\dfrac{ax}{\frac{y}{y_0}+\mathrm{e}^{\frac{-y}{y_0}}+ahx}$	Tyutyunov *et al.*, [35]
Tyutyunov function no 2	$\dfrac{ax}{\frac{y}{y_0}+\frac{1}{1+\frac{y}{y_0}}+ahx}$	Tyutyunov *et al.*, [36]

where $cov(\phi, \Phi)$ is the covariance of the rank variables, $\sigma(\phi)$ and $\sigma(\Phi)$ are the standard deviations of the rank variables.According to [17], the significance was tested using t-test:

$$t = \rho \left(\frac{n-2}{1-\rho^2} \right)^{1/2},$$

with $n - 2$ degrees of freedom under the null hypothesis.

2.4. Bootstrapping as a way to assess parameter values

Table 1 shows that the functional response, be it $\phi(x)$ or $\phi(x, y)$, and therefore $\phi(n)$, depends on a certain set of parameters. For example, the Bazykin–Crowley–Martin functional response (Tab. 1) depends on numerical values of three parameters: a, b, and h. This means that when comparing the time series $\phi(n)$ and $\Phi(n)$, the result of such a comparison can, in particular, depend on the numerical values of the parameters of the functions $\phi(x)$ and $\phi(x, y)$. To estimate the range of parameter values that results in the best match between $\phi(n)$ and $\Phi(n)$ time series, we use bootstrapping [18]. Bootstrapping is carried out in several stages:

1. Numerical values of parameters of the function $\phi(n)$ at which the minimum Euclidean norm $\|\Delta\|$ is reached are determined. Here

$$\Delta = (\Delta(1), \Delta(2)..., \Delta(n), ..., \Delta(N)). \tag{2.4}$$

   In (2.4), $\Delta(n) = \Phi(n) - \phi(n), n = 1, 2, \ldots, N$, and N is the length of the $\Phi(n)$ and $\phi(n)$ time series.
2. Then the values of $\Delta(n)$ are shuffled. The result of this shuffling is the vector

$$\Delta^* = (\Delta^*(1), \Delta^*(2)..., \Delta^*(N)).$$

3. Now, the vector

$$\Phi^* = (\phi(1) + \Delta^*(1), \phi(2) + \Delta^*(2)..., \phi(N) + \Delta^*(N)).$$

   is generated. Here, $\phi(n), n = 1, 2, \ldots, N$, is calculated for parameter values corresponding to the minimum of the Euclidean norm $\|\Delta^*\|$.
4. In the next iteration, we come back to point (2) and repeat the execution of the following points (2)–(4). Calculations stop when the relative changes in the standard deviations of parameter values distributions do not exceed a predetermined small value, namely when $\left|\frac{\sigma(k)-\sigma(k+1)}{\sigma(k)}\right| < 0.0001$, where k is the iteration number.

We used the MatLab platform to perform the calculations. In particular, the MatLab solver “fmincon” was used, which finds the minimum of a multivariable function using the “Interior-Point” algorithm.

2.5. Missing-data imputation

The raw data contained some missing data (see Supplementary information). This small number of missed data was imputed by seasonally split missing value imputation (with interpolation) using the impute TS package [37, 38]. The imputation algorithm splits the time series into seasons and afterwards performs imputation separately for each of the resulting time series datasets (each containing the data for one specific season).

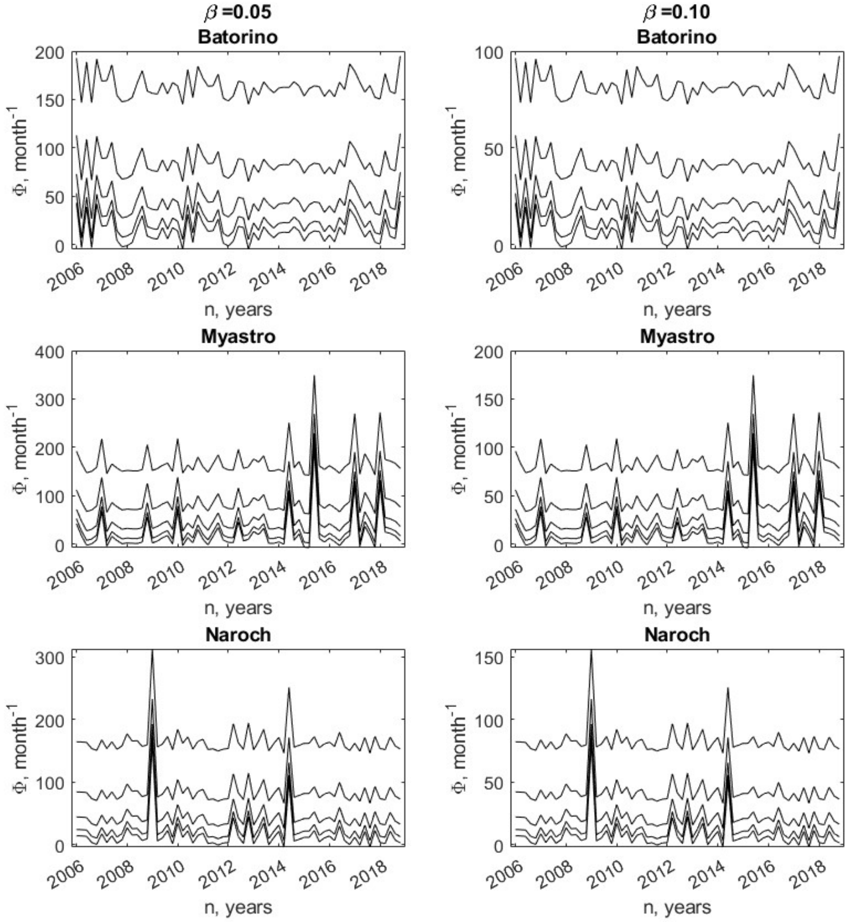

FIGURE 3. Fluctuations in the plankton functional response, $\Phi(n)$, for the Naroch Lakes (time step is 1 month); $\alpha(month^{-1}) = 0.5, 1.0, 2.0, 4.0, 8.0$ (for graphs from bottom to top); $\beta = 0.05, 0.1$. The years during which monitoring was carried out are marked under the abscissa axes. During the calculations of the plankton functional response, $\Phi(n)$, we excluded the cold period of the year for which data were not available. Thus, the calculations excluded the time step between the end of one season and the beginning of the next one.

3. RESULTS

Taking into account equation (2.2), the trophic function can be given as

$$f(n) = \frac{\Delta Z(n) + \alpha Z(n)}{\beta P(n) Z(n)}. \tag{3.1}$$

As evident from (3.1), the trophic function $f(n)$ depends on two parameters, α and β. According to Lindeman's 10 % law [39], the numerical value of β should not differ much from 0.1. The numerical values of α presented in this paper ($\alpha = 0.5, 1.0, 2.0, 4.0, 8.0$) are within the limits that correspond to the results of the monitoring of the Naroch Lakes [40]. Based on the monitoring data, *i.e.*, on the functions $P(n)$ and $Z(n)$, it is possible to obtain the dependence $f(n)$, in accordance with equation (3.1), and then determine the functional response $\Phi(n)$ as a time series, using equation (2.3) (Fig. 3).

Table 2. The correspondence of the representations of the functional response in the form of functions presented in Table 1 to the dynamics of $\Phi(n)$ in Lake Batorino ($\alpha = 4, \beta = 0.1$).

ϕ type	Label (function name)	Functional response $\phi(x)$ or $\phi(x, y)$	$\Vert\Delta\Vert$	ρ (***$p < 0.001$; **$p < 0.01$; *$p < 0.05$)	The range of parameter values that results in the best match between $\phi(n)$ and $\Phi(n)$ time series (Q1; Q3)
x, y	Bazykin–Crowley–Martin	$\frac{ax}{(1+ahx)} \cdot \frac{1}{(1+by)}$	45.161	0.435***	a (378.7;7.9E+18) h (0.0204;0.0217) b (0.0391;0.0634)
x, y	Hassell–Varley–Holling	$\frac{ax/y^m}{(1+awx/y^m)}$	47.502	0.344**	a (317.4;7044.2) w (0.0225;0.02331) m (1.0265;2.878)
x, y	Ratio–dependent Arditi–Ginzburg–Contois (AGC)	$\frac{ax/y}{(1+ahx/y)}$	48.003	0.223	a (301.22;613.82) h (0.0225;0.0232)
x, y	Tyutyunov function no 1	$\frac{ax}{\frac{y}{y_0}+\mathrm{e}^{\frac{-y}{y_0}}+ahx}$	48.003	0.223	a (2807.911;2807.948) h (0.0224;0.02314) y_0 (0.0868;0.2817)
x, y	Tyutyunov function no 2	$\frac{ax}{\frac{y}{y_0}+\frac{1}{1+\frac{y}{y_0}}+ahx}$	48.003	0.223	a (3283.95;71044.62) h (0.0223;0.0231) y_0 (0.0101;0.5036)
x, y	Beddington–DeAngelis	$\frac{ax}{(1+awy+ahx)}$	48.043	0.218	a (9997.159;9997.1601) w (0.0012;0.0032) h (0.0223;0.0231)
x, y	Ratio–dependent Ivlev	$R(1 - \mathrm{e}^{-bx/y})$	48.210	0.226	b (2.5431;3.595) R (42.2095;42.7312)
x, y	Ratio–dependent Arditi–Ginzburg	$min(ax/y, R)$	48.351	0.28	a (52.55;59.05) R (42.0640;42.2763)
x	Exponential Ivlev	$R(1 - \mathrm{e}^{-x/a})$	49.395	–0.195	a (0.162;0.9859) R (41.8624;42.3070)
x	θ-Sigmoid	$cx^\theta/(d^\theta + x^\theta)$	49.651	0.093	c (41.8583;41.8584) d (1.1455;1.2244) θ (33.8654;33.8657)
x	Sigmoid function no 1	$cx^2/(d^2 + x^2)$	49.651	–0.195	c (41.8583;42.2625) d (0.0004;0.5148)
x	Hyperbolic (Holling's disk equation)	$\alpha x/(1 + \alpha hx)$	49.651	0.098	a (387.0231;2.17E+152) h (0.0235;0.0239)
x	Sigmoid function no 2	$\frac{cx^2}{(1+bx+chx^2)}$	49.666	–0.195	c (3.37E+09;2.037E+11) b (2.62E+6;6.71E+7) h(0.0234;0.0238)
x, y	Hassell–Varley	cx/y^m	194.543	–0.113	c (2.6601;3.1792) m (0.1034;0.3576)

Table 2. continued.

x, y	Mechanistic interference	$ax/(1+awy)$	195.878	–0.159	a (2.5456;3.13547) w (1.26E-06;0.0414)
x	Linear Lotka–Volterra	αx	196.091	–0.195	a (3.44E-07;2.95E-05)
x, y	Linear interference	cx/y	236.368	0.223	c (3.29E-07;3.95E-07)
x, y	Trân function	$\frac{x}{y}\left(1-\mathrm{e}^{-\epsilon y}\right)$	303.012	0.223	ϵ (1.0E-05;1.001E-05)

Table 3. The correspondence of the representations of the functional response in the form of functions presented in Table 1 to the dynamics of $\Phi(n)$ in Lake Myastro ($\alpha = 4, \beta = 0.1$).

ϕ type	Label (function name)	Functional response $\phi(x)$ or $\phi(x, y)$	$\|\Delta\|$	ρ (***$p < 0.001$; **$p < 0.01$; *$p < 0.05$)	The range of parameter values that results in the best match between $\phi(n)$ and $\Phi(n)$ time series (Q1; Q3)
x, y	Bazykin–Crowley–Martin	$\frac{ax}{(1+ahx)} \cdot \frac{1}{(1+by)}$	108.603	0.553***	a (1274.1;2.08E+32) h (0.0103;0.0119) b (0.7789;1.0465)
x, y	Hassell–Varley–Holling	$\frac{ax/y^m}{(1+awx/y^m)}$	136.699	0.423***	a (208.189;1655.74) w (0.0195;0.0211) m (0.4836;2.2128)
x, y	Ratio–dependent Arditi–Ginzburg–Contois (AGC)	$\frac{ax/y}{(1+ahx/y)}$	136.837	0.388**	a (306.898;694.649) h (0.0199;0.0211)
x, y	Beddington–DeAngelis	$\frac{ax}{(1+awy+ahx)}$	136.837	0.388**	a (463.874;5.57E+15) w (0.001;0.0028) h (0.0194;0.0210)
x, y	Ratio–dependent Ivlev	$R(1-\mathrm{e}^{-bx/y})$	139.798	0.369**	b (8.9553;19.2384) R (45.1925;45.8142)
x	θ-Sigmoid	$cx^\theta/(d^\theta + x^\theta)$	140.061	0.068	c (45.1419;46.2388) d (0.2612;0.3333) θ (3.0829;193.7954)
x, y	Ratio–dependent Arditi–Ginzburg	$min(ax/y, R)$	140.159	0.27	a (244.204;364.589) R (45.154;45.761)
x	Exponential Ivlev	$R(1-\mathrm{e}^{-x/a})$	140.192	0.064	a (0.093;0.296) R (45.036;45.922)
x	Sigmoid function no 1	$cx^2/(d^2+x^2)$	140.603	0.068	c (44.969;45.925) d (0.00029;0.1998)
x	Sigmoid function no 2	$\frac{cx^2}{(1+bx+chx^2)}$	140.603	0.068	c (2513.637;1.77E+10) b (0.0048;652E+6) h(0.0212;0.0221)

Table 3. continued.

x, y	Tyutyunov function no 1	$\dfrac{ax}{\frac{y}{y_0}+\mathrm{e}^{\frac{-y}{y_0}}+ahx}$	141.033	0.068	a (492.508;3.07E+9) h (0.0212;0.0222) y_0 (1799.143;6.12E+6)
x, y	Tyutyunov function no 2	$\dfrac{ax}{\frac{y}{y_0}+\frac{1}{1+\frac{y}{y_0}}+ahx}$	141.033	0.068	a (517.19;1.32E+10) h (0.0213;0.022) y_0 (5012.622;6.02E+6)
x	Hyperbolic (Holling's disk equation)	$\alpha x/(1+\alpha hx)$	141.033	0.068	a (617.0903;4.43E+152) h (0.0214;0.0222)
x	Hassell–Varley	cx/y^m	307.593	0.165	c (1.4289;1.7588) m (0.4953;0.6215)
x	Linear Lotka–Volterra	αx	309.230	0.068	a (4.03E-07;4.74E-07)
x, y	Mechanistic interference	$ax/(1+awy)$	315.012	0.309*	a (9.147;15.346) w (0.6451;0.8758)
x, y	Linear interference	cx/y	333.635	0.388**	c (2.44E-07;3.02E-07)
x, y	Trân function	$\dfrac{x}{y}\left(1-\mathrm{e}^{-\epsilon y}\right)$	339.248	0.388**	ϵ (1.05E-05;1.05E-05)

Table 4. The correspondence of the representations of the functional response in the form of functions presented in Table 1 to the dynamics of $\Phi(n)$ in Lake Naroch ($\alpha = 4, \beta = 0.1$).

ϕ type	Label (function name)	Functional response $\phi(x)$ or $\phi(x, y)$	$\\|\Delta\\|$	ρ (***$p < 0.001$; **$p < 0.01$; *$p < 0.05$)	The range of parameter values that results in the best match between $\phi(n)$ and $\Phi(n)$ time series (Q1; Q3)
x, y	Bazykin–Crowley–Martin	$\dfrac{ax}{(1+ahx)}\cdot\dfrac{1}{(1+by)}$	80.883	0.567***	a (1744.18;3.46E+85) h (0.0133;0.0152) b (0.9514;1.2679)
x, y	Hassell–Varley–Holling	$\dfrac{ax/y^m}{(1+awx/y^m)}$	91.533	0.417***	a (162.457;284.34) w (0.0201;0.0217) m (1.0109;1.9325)
x, y	Beddington–DeAngelis	$\dfrac{ax}{(1+awy+ahx)}$	92.24	0.345**	a (978.489;6.18E+33) w (0.0024;0.0055) h (0.0196;0.0212)
x, y	Ratio-dependent Arditi–Ginzburg–Contois (AGC)	$\dfrac{ax/y}{(1+ahx/y)}$	92.24	0.345**	a (162.273;317.991) h (0.0198;0.0215)
x, y	Tyutyunov function no 2	$\dfrac{ax}{\frac{y}{y_0}+\frac{1}{1+\frac{y}{y_0}}+ahx}$	92.241	0.345**	a (445.533;2.26E+5) h (0.0197;0.0219) y_0 (0.093;2.21E+7)

TABLE 4. continued.

x, y	Tyutyunov function no 1	$\dfrac{ax}{\frac{y}{y_0}+\mathrm{e}^{\frac{-y}{y_0}}+ahx}$	92.241	0.345**	a (437.532;16898.13) h (0.0201;0.0218) y_0 (0.0374;1.36E+151)
x	θ-Sigmoid	$cx^\theta/(d^\theta + x^\theta)$	96.209	–0.06	c (42.592;43.329) d (0.296;0.308) θ (6.935;605.307)
x	Exponential Ivlev	$R(1 - \mathrm{e}^{-x/a})$	96.281	–0.05	a (0.0167;0.1367) R (42.5926;42.9732)
x, y	Ratio-dependent Arditi–Ginzburg	$min(ax/y, R)$	96.299	–0.047	a (104.886;126.67) R (42.592;42.657)
x, y	Ratio-dependent Ivlev	$R(1 - \mathrm{e}^{-bx/y})$	96.303	0.213	b (60.6425;60.6425) R (42.5922;42.5922)
x	Hyperbolic (Holling's disk equation)	$\alpha x/(1 + \alpha hx)$	96.303	–0.051	a (1569.253;3.33E+152) h (0.0228;0.0235)
x	Sigmoid function no 1	$cx^2/(d^2 + x^2)$	96.303	–0.051	c (42.592;42.99) d (6.36E-05;0.0755)
x	Sigmoid function no 2	$\dfrac{cx^2}{(1+bx+chx^2)}$	96.303	–0.051	c (5.95E+09;6.31E+12) b (8.43E+05;2.7E+07) h(0.0229;0.0235)
x	Hassell–Varley	cx/y^m	188.91	0.224	c (10.317;12.003) m (0.617;0.789)
x, y	Mechanistic interference	$ax/(1 + awy)$	196.004	0.263	a (71.874;143.05) w (0.0846;0.1033)
x, y	Linear interference	cx/y	201.54	0.345**	c (6.727;7.305)
x	Linear Lotka–Volterra	αx	203.188	–0.051	a (1.71E-06;2.23E-06)
x, y	Trân function	$\dfrac{x}{y}\left(1 - \mathrm{e}^{-\epsilon y}\right)$	333.432	0.345**	ϵ (9.91E-09;1.02E-08)

The irregular nature of the $\Phi(n)$ function, which is obvious from Figure 3, is due to the dependence of $\Phi(n)$ on irregular $P(n)$ oscillations (Fig. 1) and on the trophic function $f(n)$ (see (2.3)), which, in turn, as can be seen from (3.1), is related to the plankton dynamics in the ecosystem of the Naroch Lakes that have been found to be chaotic [41]. As follows from equation (3.1) (taking into account equation (2.3)) and as can be seen from Figure 3, an increase in the numerical value of the parameter α is accompanied by an increase in the functional response $\Phi(n)$, while an increase in the β value leads to a decrease in $\Phi(n)$.

Which representation of the functional response in the form of functions (Tab. 1) more accurately describes the dynamics of $\Phi(n)$? To answer this question, we use the monitoring data (Figs. 1 and 2). In particular, we substitute monitoring data, *i.e.*, the time series of phytoplankton $P(n)$ and zooplankton $Z(n)$, into the formulas from Table 1), where $x \to P(n), y \to Z(n)$, resulting in the time series $\phi(n)$. Then we numerically estimate the norm $\|\Delta\|$, *i.e.*, the level of proximity between the $\phi(n)$ and $\Phi(n)$ time series (for more information see description of methods in Section 2. The results for fixed values of the parameters α and β ($\alpha = 4, \beta = 0.1$) of the model (2.1)–(2.2) are shown in Tables 2–4. In Supplementary Information, the results are presented more broadly (including for other values of the parameters α and β). The sensitivity of our results to variations in the numerical values of these parameters is also briefly discussed in the Discussion section.

As can be seen from Tables 2–4, the norm $\|\Delta\|$ takes the minimum values for the Bazykin–Crowley–Martin functional response. In other words, it is the predator-dependent Bazykin–Crowley–Martin functional response that best matches the monitoring data. It should be noted that the same Bazykin–Crowley–Martin functional response characterizes the phytoplankton-zooplankton relationship in each of the lakes even though the trophic states of the water bodies in the Naroch Lakes ecosystem differ significantly [42]; see Supplementary Information.

It can be seen that the ranges of parameter values that lead to the best match between the time series $\phi(n)$ and $\Phi(n)$ can differ significantly depending on the selected parameter of $\phi(n)$. For example, the distribution of values of parameter a of the Bazykin–Crowley–Martin function is characterized by a very large difference between the numerical values of the first and third quartiles ($Q1 = 1744.1770$ and $Q3 = 3.46E + 85$), while the corresponding values for parameter h lie in a much narrower range, between $Q1 = 0.0133$ and $Q3 = 0.0152$ (Tab. 4, Lake Naroch). We also note the fact that there are predator-dependent functional responses, for which the numerical values of $\|\Delta\|$, although exceeding the numerical value of $\|\Delta\|$, which characterizes the Bazykin–Crowley–Martin functional response, do not exceed the values of $\|\Delta\|$ for prey-dependent functional responses. The comparison of the prey-dependent functional responses and the predator-dependent functional responses (shown in Tab. 1) reveals that

$$min\|\Delta\|(prey - dependent) > min\|\Delta\|(predator - dependent)$$

for all the water bodies of the Naroch Lakes ecosystem (see Tabs. 2–4, and also Supplementary Information). In order to make clear the correspondence or non-correspondence of the time series of $\phi(n)$ to the time series $\Phi(n)$, we use scatter plots where the numerical values of $\phi(n)$ are presented in comparison with the numerical values of $\Phi(n)$. Examples of such scatter plots for three time series $\phi(n)$ and $\Phi(n)$ are shown in Figure 4.

As can be seen from Figure 4, the scatter plots for the prey-dependent Hyperbolic function (see Tab. 1) represent narrow stripes parallel to the abscissa $\Phi(n)$ axes. This means that very close, almost the same values of $\phi(n)$ correspond to a wide range of values of $\Phi(n)$. Numerically, this leads to a very weak and statistically insignificant correlation (*i.e.*, in fact, to its absence) between the time series $\phi(n)$ for the Hyperbolic functional response and $\Phi(n)$ (see Tabs. 2–4). Note that (Fig. 4), although less pronounced, the sections of scatter plots that are parallel to the abscissa axes are also characteristic of the predator-dependent Arditi–Ginzburg–Contois response in Lake Myastro and Lake Naroch (Fig. 4). The correlation coefficients between $\phi(n)$ and $\Phi(n)$ time series therewith are lower than those for the predator-dependent Bazykin–Crowley–Martin functional response, where there are no similar sections (Fig. 4), but noticeably exceed the correlation coefficients for the prey-dependent hyperbolic functional response (Tabs. 2–4). In Lake Myastro and Lake Naroch, the increase in numerical values of $\Phi(n)$ is basically accompanied by an increase in $\phi(n)$ for the Bazykin–Crowley–Martin function (Fig. 4), which is reflected in a statistically significant correlation between time series $\phi(n)$ and $\Phi(n)$ (Tabs. 3 and 4). The scatter plots characteristic of Lake Batorino for the Bazykin–Crowley–Martin and Arditi–Ginzburg–Contois functional responses demonstrate much less noticeable growth of $\phi(n)$ values with increasing values of $\Phi(n)$ (Fig. 4). As a result, the correlation between $\phi(n)$ and $\Phi(n)$ decreases compared to the correlation between these time series in Lake Naroch and Lake Myastro for the Bazykin–Crowley–Martin function, and the correlation between $\phi(n)$ and $\Phi(n)$ for the Arditi–Ginzburg–Contois function becomes statistically unreliable.

The above results are obtained for fixed parameter values of the model (2.1)–(2.2) ($\alpha = 4, \beta = 0.1$). The question naturally arises as to how sensitive these results are to parameter α and β variations. The results of evaluating the effects associated with changes in the numerical values of α and β are presented in Supplementary Information. One can see that it is the Bazykin–Crowley–Martin function that best corresponds to the functional response $\Phi(n)$ when changing the numerical values of the parameters α and β. The only exception is at $\alpha = 0.5, \beta = 0.1$, when the functional response $\Phi(n)$ is best matched by the Hassell–Varley function. However, in this case, despite the fact that the norm for the Bazykin–Crowley–Martin function is slightly higher than for

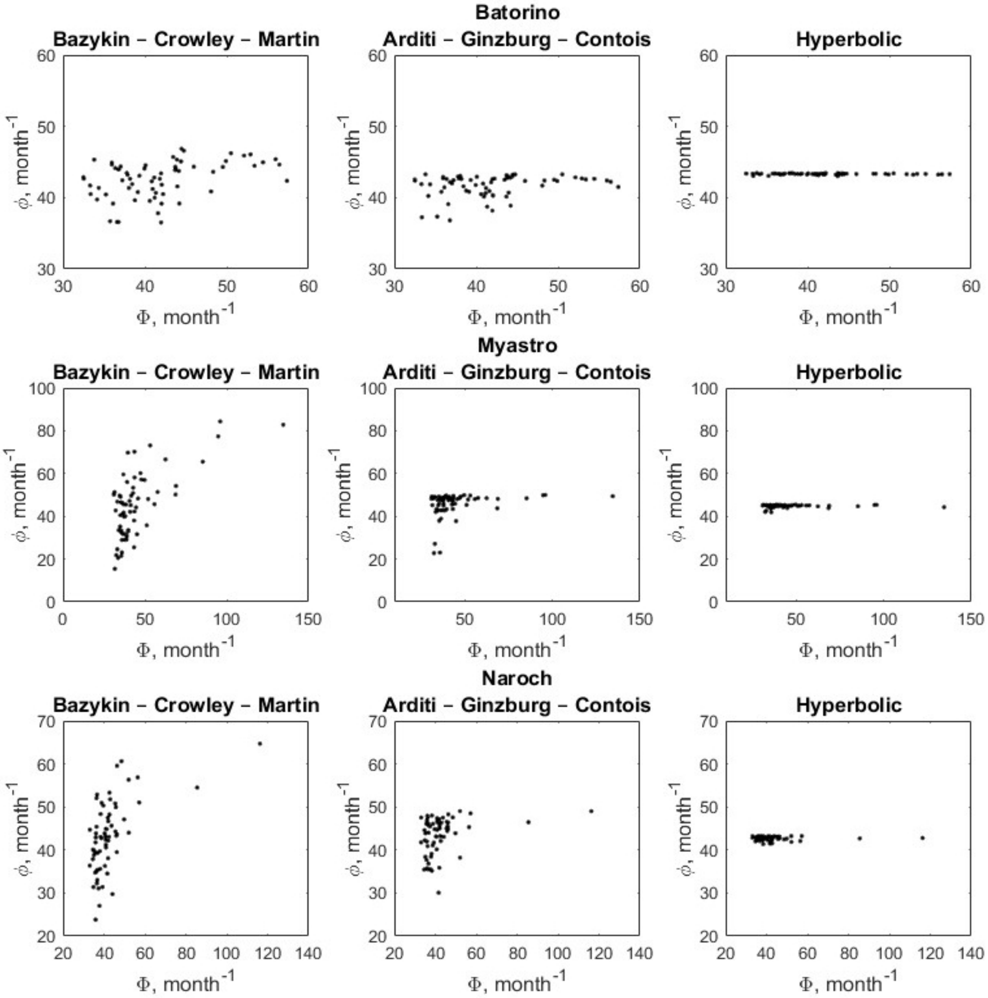

Figure 4. The scatter plots $\phi(n)$ vs $\Phi(n)$ in each of the water bodies of the Naroch Lakes ecosystem for the Bazykin–Crowley–Martin functional response ($a = 4843.320, h = 0.014, b = 1.090$ for Lake Naroch; $a = 9998.380, h = 0.011, b = 0.850$ for Lake Myastro; $a = 4612.830, h = 0.021, b = 0.050$ for Lake Batorino), the Arditi–Ginzburg–Contois functional response ($a = 205.660, h = 0.020$ for Lake Naroch; $a = 429.220, h = 0.020$ for Lake Myastro; $a = 402.290, h = 0.023$ for Lake Batorino), and the Hyperbolic functional response ($a = 2764.190, h = 0.023$ for Lake Naroch; $a = 1619.400, h = 0.022$ for Lake Myastro; $a = 1939.160, h = 0.023$ for Lake Batorino).

the Hassell – Varley function, the correlation for the Bazykin–Crowley–Martin function remains the highest at $\alpha = 0.5, \beta = 0.1$.

4. Discussion

Trophic relationships involving resource consumption, which depends both on the properties of the resource consumed and on the characteristics of the animals that are consumers, are one of the most important ecological processes [22]. Such relationships are often analyzed using mathematical models describing interactions such as “predator-prey” or “resource-consumer”. Within the framework of the KD approach, the functions describing the processes that determine the dynamics of prey and predator populations are set *a priori*. An example of such functions is the functions $G(x)$, $F_1(x, y)$ in equation (1.1) and $F_2(x, y)$ in equation (1.2). The specific type of such functions is largely determined by the views of researchers on the nature of the processes they study. In particular, the choice between a prey-dependent functional response $\phi(x)$ and a predator-dependent functional response $\phi(x, y)$ has been the subject of intense debate [4, 43].

In the context of the KDD approach [13], it turned out that the predator-dependent Bazykin–Crowley–Martin function best corresponds to the results of the monitoring of the ecosystem of the Naroch Lakes. It should be noted that parameter a of this function for each of the water bodies of the Naroch Lakes system is defined in extremely wide limits (Tabs. 2–4). However, since the comparatively small numerical values of parameter h can vary in relatively narrow ranges (Tabs. 2–4), the first multiplier of the Bazykin–Crowley–Martin function (and, consequently, this function as a whole) turns out to be extremely weakly dependent on the choice of the value of parameter a. As a result, the numerical values of the norm characterizing the proximity of the time series $\Phi(n)$ and $\phi(n)$ vary extremely slightly in the predominant part of the wide range of changes in parameter a.

As can be seen from Tables 2–4, bootstraping does not impose restrictions on the parameters of the functional response, which, like parameter a of the Bazykin–Crowley–Martin function, determine the searching rate. In other words, the numerical values of these parameters, being practically unidentifiable, can vary over a wide range, having little effect on the estimate of the proximity of the time series $\Phi(n)$ and $\phi(n)$. Naturally, the question arises whether such a result is a feature of the method we use to estimate the range of changes in model parameters, or whether it objectively reflects the weak dependence of the searching rate on dynamics in the form of time series resulting from monitoring the lake ecosystem. In this context, in a future study, a comparison of different methods, such as bootstraping, least-squares fitting, maximum-likelihood, profile likelihood or Bayesian MCMC, could be of significant interest.

Since the monitoring results, *i.e.* the time series $P(n)$ and $Z(n)$, are influenced by many different biotic and abiotic factors, these time series reflect not only the prey–predator interaction, but also temporary changes in the lake ecosystem as a whole. For the same reason, the time series $\Phi(n)$ holistically characterizes the entire ecosystem of each of the lakes.

The Bazykin–Crowley–Martin time series obtained taking into account the results of monitoring the ecosystem of the Naroch Lakes, mirrors the impact of a huge variety of factors on plankton dynamics and, in this sense, are holistic in nature. Taking into account this circumstance, as well as the fact that the Bazykin–Crowley–Martin function allows for the mutual interference of predators/zooplankters, the question arises whether the range of changes in the numerical value of parameter b, characterizing the interference of zooplankters, depends on such an integral characteristic as the trophic status of the water bodies of the Naroch Lakes ecosystem. The importance of raising this question is determined by the fact that these water bodies have different trophic status [42] (see also Supplementary Information), even though they are interconnected and in close proximity to each other.

The difference in trophic status may cause significant differences in the level of interference. In particular, in a resource-rich eutrophic reservoir, interference between zooplankters due to their competition for a resource, phytoplankton, should probably be less than, for example, in an oligotrophic reservoir, which is characterized by a reduced phytoplankton number.

Table 5 shows that the numerical values of Q_1 and Q_3 decrease monotonically from the oligo-mesotrophic Lake Naroch to the mesotrophic Lake Myastro and then to the eutrophic Lake Batorino. This means that parameter b of the Bazykin–Crowley–Martin function can effectively reflect the correspondence of the level of interference between zooplankters to the trophic status of the whole water body system.

In light of the obtained results, we emphasize a qualitative difference of the Bazykin–Crowley–Martin functional response from the other considered predator-dependent functions, which consists in its ability to account implicitly for various factors that may limit the consumer's reproduction beside availability of the food. This property manifests itself as saturation of the non-trivial zero-isocline of the predator equation in the Gause–Kolmogorov model with constant natural mortality of predator. The isocline is defined on the phase plane (x, y) by implicit equation $\phi(x, y) = \alpha/\beta$. Figure 5 presents the predator zero-isoclines built for BCM, AGC, and HVH functional responses with parameter values estimated for lakes Batorino, Myastro, and Naroch (the respective

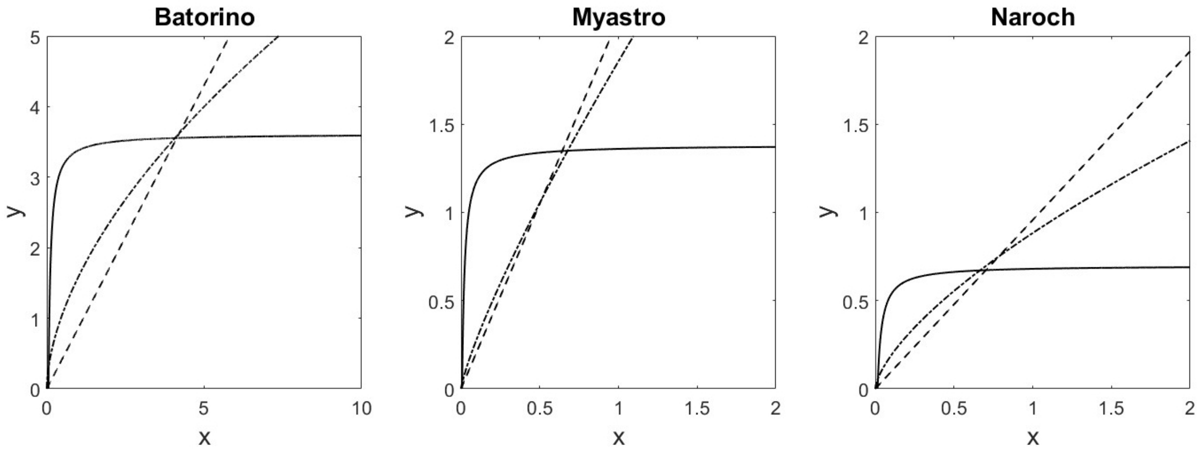

FIGURE 5. Predator zero-isoclines of the Gause–Kolmogorov model built for three different predator-dependent functional responses for trophic system in lakes Batorino, Myastro, and Naroch (BCM is the solid line. AGC is the dotted line, HVH is the dashed dotted line). The following numerical values of the parameters were used:($\alpha = 4, \beta = 0.1; a = 4612.83, h = 0.021069, b = 0.051653$ (BCM, Lake Batorino); $a = 407.8458, h = 0.022889$ (AGC, Lake Batorino); $a = 1094.46, w = 0.022968, m = 1.737267$ (HVH, Lake Batorino); $a = 9998.38, h = 0.01115676, b = 0.89765292$ (BCM, Lake Myastro); $a = 488.638625, h = 0.02070771$ (AGC, Lake Myastro); $a = 466.687472, w = 0.0204337, m = 1.2229976$ (HVH, Lake Myastro); $a = 6219.177, h = 0.014097, b = 1.107792$ (BCM, Lake Naroch); $a = 225.0187, h = 0.020748$ (AGC, Lake Naroch); $a = 211.4874, w = 0.021072, m = 1.488577$ (HVH, Lake Naroch).

TABLE 5. Q_1 and Q_3 for distributions of the parameter b of the Bazykin–Crowley–Martin function numerical values depending on α and β for each of the water bodies of the Naroch Lakes ecosystem

α	β	Lake Naroch Oligo-mesotrophic		Lake Myastro Mesotrophic		Lake Batorino Eutrophic	
		Q_1	Q_3	Q_1	Q_3	Q_1	Q_3
8	0.1	0.2598	0.3639	0.1520	0.2060	0.02	0.0301
4	0.1	0.9514	1.2679	0.7789	1.0465	0.0391	0.0634
2	0.1	8.8568	12.3247	4.2219	5.4175	0.0992	0.1546
1	0.1	2078.360	25883.5611	11.5657	19.8517	0.2729	0.4797
8	0.05	0.2644	0.3699	0.1472	0.2020	0.0184	0.0277
4	0.05	0.9193	1.3062	0.7821	1.0357	0.0419	0.0631
2	0.05	9.1179	12.4259	4.1807	5.4631	0.0989	0.1524
1	0.05	2449.079	22453.5362	13.6148	21.3984	0.2796	0.4743

data is given in Tables S4, S14, and S24 of Supplementary Information). One can easily notice the difference between these three zero-isoclines. The isocline of the Arditi–Ginzburg–Contois functional response is a straight line passing through the origin, the isocline of the Hassel–Varley–Holling function is presented by the concave unboundedly growing curve, also crossing the origin. The isocline corresponding to the Bazykin–Crowley–Martin function crosses the abscissa axis at positive value of x, saturating with prey density. This saturation reveals that growth of zooplankton can be limited by other factors besides the phytoplankton density [44]. Earlier studies [5, 13] suggest that abiotic factors, in particular temperature oscillations, can play an important role, determining plankton dynamics particularly, in the ecosystem of the Naroch Lakes).

Our results support theoretical principles formulated by Arditi and Ginzburg [4, 31, 45] who suggested to use the simplest predator-dependent functional response, the ratio-dependent function, which has only two parameters similar to those of the Holling's disk equation, as a null model of predator interference. In this regard, it seems to us that the point of view of Ginzburg and Damuth ("The issue isn't which model of consumer interference is right, but which one is least wrong"), clearly presented directly in the title of their article [46], is reasonable. Depending on the practical needs and the availability of observed data, the more detailed models can be built on this theoretical basis. In our case, the Arditi–Ginzburg–Contois functional response has demonstrated fairly good fitting to observations among the other popular predator–dependent models (see Tabs. 2–4 and Tables S3–S32 in Supplementary Information). A more elaborate study based on the knowledge-and-data driven, or KDD, approach allowed us to identify such a function, namely the Bazykin–Crowley–Martin function, describing the functional response of zooplankton, which best corresponds to the functional response $\Phi(n)$ allowing for the specifics of plankton dynamics in the Naroch Lakes. Thus, the KDD approach can be a useful addition to those methods of mathematical modeling that have been used so far.

Acknowledgments

We would like to thank the anonymous reviewers for reading and commenting on an earlier version of this paper. The authors thank the researches and technicians of the Research Laboratory of Aquatic Ecology and the Naroch Biological Station of the Belarusian State University who carried out monitoring of the Naroch Lakes.

Funding

The reported study was funded by the Russian Science Foundation, Grant Number 23-24-00408.

Data availability statement

The research data associated with this article are included in the article.

Supplementary Material

Supplementary Information is available at https://www.mmnp-journal.org/10.1051/mmnp/2025014/olm

References

[1] B.A. Maurer, Untangling ecological complexity. The Macroscopic Perspective. The University of Chicago, Chicago (1999).

[2] P. Turchin, Complex population dynamics. A Theoretical/Empirical Synthesis. Princeton University, Princeton (2003).

[3] R.V. Sole and J. Bascompte, Self-organization in Complex Ecosystems. Princeton University, Princeton (2006).

[4] R. Arditi and L.R. Ginzburg, How species interact. Altering the Standard View of Trophic Ecology. Oxford University, New York (2012).

[5] A.B. Medvinsky, B.V. Adamovich, A.V. Rusakov, D.A. Tikhonov, N.I. Nurieva and V.M. Tereshko, Population dynamics: mathematical modeling and reality. *Biophysics* **64** (2019) 956–977.

[6] P. Yodzis, Diffuse effects in food webs. *Ecology* **81** (2000) 261–266.

[7] G.F. Gause, The Struggle for Existence. Williams & Wilkins, Baltimore (1934).

[8] A.N. Kolmogoroff, Sulla teoria di Volterra della lotta per l'esistenza. *Giornale Inst. Ital. Attuari* **7** (1936) 74–80 (in Italian).

[9] A.N. Kolmogorov, Qualitative study of mathematical models of population dynamics. *Probl. Kibernet.* **25** (1972) 100–106 (in Russian).

[10] A. Majumder, D. Adak and N. Bairagi, Persistence and extinction of species in a disease-induced ecological system under environmental stochasticity. *Phys. Rev. E* **103** (2021) 032412.

[11] A. Majumder, D. Adak and N. Bairagi, Phytoplankton-zooplankton interaction under environmental stochasticity: survival, extinction and stability. *Appl. Math. Model.* **89** (2021) 1382–1404.

[12] D. Pattanayak, A. Mishra, S.K. Dana and N. Bairagi, Bistability and tri-trophic food chain model: basin stability perspective. *Chaos* **31** (2021) 073124.

[13] A.B. Medvinsky, N.I. Nurieva, B.V. Adamovich, N.P. Radchikova and A.V. Rusakov, Direct input of monitoring data into a mechanistic ecological model as a way to identify the phytoplankton growth-rate response to temperature variations. *Sci. Rep.* **13** (2023) 10124.

[14] A.V. Rusakov, B.V. Adamovich, N.I. Nurieva, R.Z. Kovalevskaya, T.M. Mikheyeva, N.P. Radchikova, H.A. Zhukava, Y.K. Veres, T.V. Zhukova and A.B. Medvinsky, Phase synchronization of chlorophyll and total phosphorus oscillations as an indicator of the transformation of a lake ecosystem. *Sci. Rep.* **12** (2022) 11979.

[15] T.L. Rogers, B.J. Johnson and S.B. Munch, Chaos is not rare in natural ecosystems. *Nat. Ecol. Evol.* **6** (2022) 1105–1111.

[16] T.L. Rogers, S.B. Munch, S.-i. Matsuzaki and C.C. Symons, Intermittent instability is widespread in plankton communities. *Ecol. Lett.* **26** (2023) 470–481.

[17] M. Pagano and K. Gauvreau, Principles of Biostatistics. 2nd edn. CRC Press, Taylor & Francis Group, New York (2018).

[18] B. Efron and R.J. Tibshirani, An Introduction to the Bootstrap. Chapman and Hall, London (1993).

[19] A.J. Lotka, Analytical note on certain rhythmic relations in organic systems. *Proc. Natl. Acad. Sci. U.S.A.* **6** (1920) 410-415.

[20] V. Volterra, Variazioni e fluttuazioni del numero d'individui in spacie animali conviventi. *Mem. Reale Accad. Nazionale Lincei* **2** (1926) 31–113 (in Italian).

[21] C.S. Holling, The functional response of predators to prey density and its role in mimicry and population regulation. *Mem. Entomol. Soc. Canada* **45** (1965) 5–60.

[22] V.S. Ivlev, Experimental Ecology of Feeding Fishes. Yale University, New Haven (1961).

[23] M.P. Hassell, The Dynamics of Arthropod Predator–Prey Systems. Princeton University, Princeton (1978).

[24] M.P. Hassell and G.C. Varley, New inductive population model for insect parasites and its bearing on biological control. *Nature* **223** (1969) 133–136.

[25] W.J. Sutherland, Aggregation and the "ideal free" distribution. *J. Anim. Ecol.* **52** (1983) 821–828.

[26] R. Arditi and H.R. Akçakaya, Underestimation of mutual interference of predators. *Oecologia* **83** (1990) 358–361.

[27] J.R. Beddington, Mutual interference between parasites or predators and its effect on searching efficiency. *J. Anim. Ecol.* **44** (1975) 331–340.

[28] D.L. DeAngelis, R.A. Goldstein and R.V. O'Neill, A model for trophic interaction. *Ecology* **56** (1975) 881–892.

[29] L.R. Ginzburg, Y.I. Goldman and A.I. Railkin, Matematicheskaya model vzaimodeistviya dvukh populyaciy. *Zh. Obshchey Biol.* **32** (1971) 724–730 (in Russian).

[30] R. Arditi, J.M. Abillon and J. Viera da Silva, A predator-prey model with saturation and intraspecific competition. *Ecol. Model.* **5** (1978) 173–191.

[31] R. Arditi and L.R. Ginzburg, Coupling in predator–prey dynamics: ratio-dependence. *J. Theor. Biol.* **139** (1989) 311–326.

[32] A.D. Bazykin, F.S Berezovskaya, G.A. Denisov, G.A. and Yu.A. Kuznetsov, The influence of predator-prey saturation effect and competition among predators. *Ecol. Model.* **14** (1981) 39–57.

[33] P.H. Crowley, and E.K. Martin, Functional responses and interference with and between year classes of a dragonfly population. *J. North Am. Benthol. Soc.* **8** (1989) 211–221.

[34] J.K. Trân, A predator–prey functional responses incorporating indirect interference and depletion. *Verhand. Int. Verein Limnol.* **30** (2008) 302–305.

[35] Yu.V. Tyutyunov, L. Titova and R. Arditi, Predator interference emerging from trophotaxis in predator–prey systems: An individual-based approach. *Ecol. Complex.* **5** (2008) 48–58.

[36] Yu.V. Tyutyunov, L.I. Titova, F.A. Surkov and E.N. Bakaeva, Trophic function of phytophagous rotifers (Rotatoria). Experiment and modelling. *Zh. Obshchey Biol.* **71** (2010) 52–62 (in Russian).

[37] M. Steffen and T. Bartz-Beielstein, Time series missing data imputation in R. *R J.* **9/1** (2017) 207–218.

[38] R Core Team, Language and Environment for Statistical Computing. R Foundation for Statistical Computing, Vienna (2018).

[39] R.L. Lindeman, The trophic-dynamic aspect of ecology. *Ecology* **23** (1942) 399–417.

[40] G.G. Winberg, G.A. Pechen and E.A. Shushkina, Production of plankton crustaceans in three lakes of different types. *Zool. Zh.* **44** (1965) 676–687 (in Russian).

[41] A.B. Medvinsky, B.V. Adamovich, A. Chakraborty, E.V. Lukyanova, T.M. Mikheyeva, N.I. Nurieva, N.P. Radchikova, A.V. Rusakov and T.V. Zhukova, Chaos far away from the edge of chaos. A recurrence quantification analysis of plankton time series. *Ecol. Compl.* **23** (2015) 61–67.

[42] B.V. Adamovich, T.V. Zhukova, T.M. Mikheyeva, R.Z. Kovalevskaya, T.A. Makarevich and A.A. Zhukova, Eutrophication, oligotrophication, and benthification in Naroch Lakes: 40 years of monitoring. *J. Siber. Fed. Univ. Biol.* **10** (2017) 379–394 (in Russian).

[43] Yu.V. Tyutyunov and L.I. Titova, From Lotka–Volterra to Arditi–Ginzburg: 90 years of evolving trophic functions.*Zh. Obshchey Biol.* **79** (2018) 428–448 (in Russian).

[44] M. Begon, J.L. Harper and C.R. Townsend, Ecology: Individuals, Populations and Communities. Blackwell Scientific Publications, Oxford (1986).

[45] R. Arditi and L.R. Ginzburg, Improving communications between theoretical ecologists, mathematical ecologists, and ecological modelers: response to the critique of our book How species interact. *Theor. Ecol.* **7** (2014) 21–22.

[46] L.R. Ginzburg and J. Damuth, The issue isn't which model of consumer interference is right, but which one is least wrong. *Front. Ecol. Evol.* **10** (2022) 860542.